

From the 2D graphene honeycomb lattice to 1D nanoribbons: dimensional crossover signals in the structural thermal fluctuations

S. Costamagna^{1,2} and A. Dobry²

¹*International School for Advanced Studies (SISSA), Via Bonomea 265, I-34136 Trieste, Italy.*

²*Facultad de Ciencias Exactas Ingeniería y Agrimensura, Universidad Nacional de Rosario and Instituto de Física Rosario, Bv. 27 de Febrero 210 bis, 2000 Rosario, Argentina.*

(Dated: June 20, 2018)

We study the dimensional crossover from 2D to 1D type behavior, which takes place in the thermal excited rippling of a graphene honeycomb lattice, when one of the dimensions of the layer is reduced. Through a joint study, by Monte Carlo (MC) atomistic simulations using a quasi-harmonic potential and analytical calculations, we find that the normal-normal correlation function does not change its power law behavior in the long wavelength limit. However the system size dependency of the square of out of plane displacement $\langle h^2 \rangle$ changes its scaling behavior when going from a layer to a nanoribbon. We show that a new scaling law appears which corresponds to a truly 1D behavior and we estimate the ratio of the sample dimensions where the crossover takes place as $R_{2D \leftrightarrow 1D} \approx 1.609$. Having explored a wide number of realistic systems sizes, we conclude that narrow ribbons present stronger corrugations than the square graphene sheets and we discuss the implications for the electronic properties of freestanding graphene systems.

PACS numbers: 73.23.-b, 73.21.La, 72.15.Qm, 71.27.+a

Introduction. The very existence of graphene¹, a first truly two dimensional crystal, is surprising because crystalline order is not expected to be possible in a two dimensional world. This is a consequence of a Mermin-Wagner theorem² which forbids the ability of any continuous symmetry breaking, the translational one in this case, in two dimensions. However, graphene exists because the atoms can explore the other dimension by moving perpendicular to the sheet direction. In fact, the stability of a two-dimensional crystalline membrane embedded in a three dimensional world has been studied extensively in connection to biological membranes³. It has been concluded that the anharmonic coupling between the in plane and the out of plane phonons stabilizes an asymptotically flat phase but strongly corrugated by the presence of ripples, whose manifestation is the divergence of the mean square of the displacement perpendicular to the sheet in the thermodynamical limit. The recently experimental demonstration of the existence of intrinsic ripples⁴ in graphene has revived this subject of study. Moreover, numerical simulations using a realistic C-C interatomic potential supports the adequacy of the scaling theory of membranes in the continuum medium approach for graphene⁵⁻⁷. The connection of these ripples and their fluctuations with the electronic transport properties is a subject of great interest nowadays⁸.

In addition to graphene sheets, ribbons where electrons are confined in the nano scale in the transversal direction, has been the subject of a lot of interest. The reason is that the lateral confinement may induce the presence of a gap in the electronic spectrum which is essential for many future nanoelectronics applications. However, the current success for the synthesis of the semiconducting graphene-based nanoribbons is still far below the expectations. Lithographic patterning of graphene into nan-

odimensions has difficulties in controlling the nanopattern size and edge qualities. It is expected that these difficulties will be overcome in the near future. Therefore prediction of the structural stability as well its interplay with the electronic transport of graphene nanoribbons is strongly desirable.

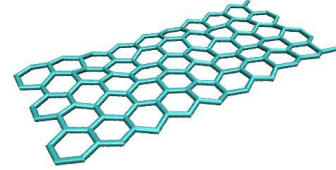


FIG. 1: Esquematic view of the corrugated graphene honeycomb lattice. The dimensions of the flat sample are given by $L_x = 3l_x a_0$ and $L_y = \sqrt{3}l_y a_0$, where $a_0 = 1.42\text{\AA}$ is the graphene lattice constant and, l_x (l_y) is the number of cells in the armchair (zigzag)-type edge. The total number of Carbon atoms is $N = 4l_x l_y$. For this example $l_x = 3$ and $l_y = 10$ and hence $N = 120$.

In this letter, we study the structural stability of graphene ribbons, extending the previous analysis conducted for the case of a square layer⁶. From the elasticity theory and using the Self Consistent Screening Approximation (SCSA) to account for the coupling between in and out of plane phonons, we analyze the dimensional crossover which takes place when one of the dimensions of a layer is reduced. The normal-normal correlation function retains its power law behavior in the long wavelength limit. However, the mean square of the height fluctuation diverges with the length of the ribbons signaling an instability for the case of thin ribbons. We check this prediction by numerical simulations with the Montecarlo method using a phenomenological quasiharmonic poten-

tial. We conclude that ribbons should be strongly more rippled as compared with layer.

Stability condition from the elasticity theory. Let $h(x, y)$ be the measure of the out-of-plane displacement of a particle sited at the (x, y) point, in a flat configuration, of a membrane. Then, the total bending energy is given by

$$E_0 = \int_{-\frac{L_x}{2}}^{\frac{L_x}{2}} dx \int_{-\frac{L_y}{2}}^{\frac{L_y}{2}} dy \left[\kappa (\nabla^2 h(x, y))^2 \right] \quad (1)$$

where κ is the bending rigidity. We are interested in comparing the case $L_x = L_y$ which represents a 2D membrane with the one $L_y \gg L_x$ corresponding to a ribbon running in the y -direction. It is convenient to bring eq.(1) to the momentum space formulation

$$E_0 = \sum_{\mathbf{k} = -(\Lambda_x, \Lambda_y)}^{(\Lambda_x, \Lambda_y)'} (|\mathbf{k}|^2)^2 |h(\mathbf{k})|^2 \quad (2)$$

where $\mathbf{k} = (k_x, k_y)$ is the two dimensional momentum vector given as $k_i = \frac{2\pi}{L_i} n_i$, $i = x, y$ in terms of the integer summation indexes n_i . Note that this supposes periodic boundary condition (PBC) in both directions. We will also use PBC in the Montecarlo simulations we will show in the next Section. Therefore, we take into account only the bulk excitations within the ribbon. The values of the width that make the ribbon unstable toward the thermally excited rippling should be taken as an upper limit of stability. Edge excitations, which are not taken into account in our approach, could destroy even thicker ribbons than which we consider here. In eq. (2) $\Lambda_x(\Lambda_y)$ is the short distance ultraviolet cutoff of the order of the inverse of the lattice constants $a_x(a_y)$. The prime over the summation sign indicates that the $(0, 0)$ point should be excluded because it corresponds to a rigid translation. The size dependency we are interested in will be related to this low momenta limit that appears in all the k -summation.

The stability of this system can be analyzed according to the size dependency of $\langle h^2 \rangle$ the mean square of the height and $\langle \theta^2 \rangle \approx \langle |\nabla h|^2 \rangle$ the one of the bending angle formed by the normal to the surface at a point with the global z -axis. For the isotropic membrane ($L = L_x = L_y$) we obtain for these quantities

$$\langle h^2 \rangle = \frac{1}{4\pi} \int_{\frac{2\pi}{L}}^{\Lambda} dk k H(k) \sim L^2, \quad \langle \theta^2 \rangle \sim \log L \quad (3)$$

where we have introduced the height-height correlation function given by $H(k) = \langle h(\mathbf{k})h(-\mathbf{k}) \rangle = \frac{1}{2\beta\kappa k^4}$.

Note that this harmonic treatment predicts a logarithmic divergence with the system size which is interpreted as a crumpled instability. Moreover, as we discuss later this instability is cured by anharmonic interactions with the in plane phonons. Before this, let us compare

with the situation of a thin ribbon ($L_y \gg L_x$). In this case the spectrum of the bending phonons $\omega_{ben}^2 = \kappa \mathbf{k}^4 = \kappa \left[\left(\frac{2\pi}{L_x} n_x \right)^2 + \left(\frac{2\pi}{L_y} n_y \right)^2 \right]^2$ is dominated by the $n_x = 0$ term. Equation (3) now takes the form

$$\langle h^2 \rangle = \frac{1}{4L_x \pi \beta \kappa} \int_{\frac{2\pi}{L_y}}^{\Lambda_y} \frac{dk_y}{k_y^4} \sim \frac{L_y^3}{L_x}, \quad \langle \theta^2 \rangle \sim \frac{L_y}{L_x} \quad (4)$$

The instability here is of course more severe than in the 2D case. This is the first indication that thin ribbons are much more sensitive to thermal out plane fluctuation than a square membrane.

However, the bending modes are coupled to the in-plane ones. A simple way to include this coupling is by taking into account that in the elastic two dimensional theory given by the energy

$$E_{pl} = \int_{-\frac{L_x}{2}}^{\frac{L_x}{2}} dx \int_{-\frac{L_y}{2}}^{\frac{L_y}{2}} dy [2\mu u_{ij}^2 + \lambda u_{ii}^2] \quad (5)$$

the strain tensor u_{ij} should include a quadratic term in h (λ is the lame constant and μ the the shear modulus). Their lowest order is therefore given by

$$u_{ij} = \frac{1}{2} [(\partial_j u_i + \partial_i u_j) + \partial_i h \partial_j h] \quad (6)$$

u_i are the x and y Cartesian components of the displacements from the equilibrium situation.

The simplest but otherwise precise treatment as compared with the Montecarlo numerical simulation⁶ is the Self Consistent Screening Approximation (SCSA) of LeDoussal and Radzihovsky⁹. The in-plane phonons are integrated out in the partition function, generating an effective quartic interaction between the out of plane modes. The correlation function $H(\mathbf{k})$ acquires a self-energy correction $H^{-1}(\mathbf{k}) = \kappa k^4 + \Sigma(\mathbf{k})$ which is self-consistently determined. The resulting coupled integral equations could be analytically solved in the long wavelength limit under the assumption $H^{-1} \approx \Sigma(\mathbf{k}) = Z k^{4-\eta}$ Z is a non universal amplitude and $\eta \approx 0.821$ is obtained by solving analytically the integrals in terms of the Γ function. A crucial point for the present analysis is that η cannot not depend on the system size (at least for big enough systems), because the integral in k involved in its calculation is convergent with the low momenta infrared limit. Therefore, we expect that η will not change when we go from a square membrane to a ribbon. This will be checked by Monte Carlo(MC) simulations.

Coming back to the membrane and including the renormalization of $H^{-1}(\mathbf{k})$ given by the SCHA, Eq. (3) becomes

$$\langle h^2 \rangle = \frac{1}{4\pi\beta\kappa} \int_{\frac{2\pi}{L}}^{\Lambda} \frac{dk}{k^{3-\eta}} \sim L^{2-\eta}, \quad \langle \theta^2 \rangle \sim L^{-\eta} \quad (7)$$

The bending angle converges for $L \rightarrow \infty$ implying a long range order on the normals. However $\langle h^2 \rangle$ diverges

which is interpreted as the origin of a strong rippling of the membrane which in fact observed in suspended graphene samples.

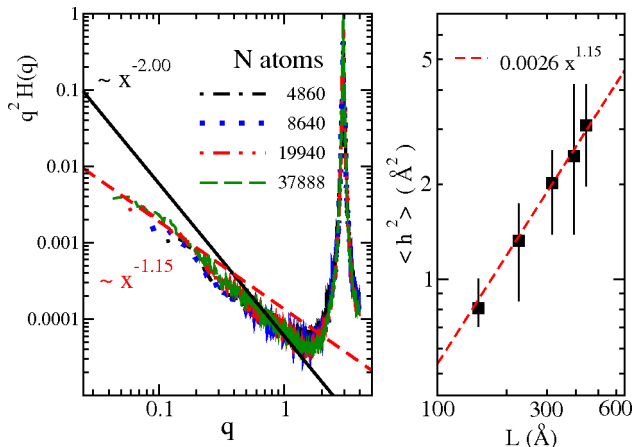


FIG. 2: (a) (Color online) $q^2 H(q)/N$ against q at $T = 300$ K for different 2D system sizes as indicated on the plot. The dashed lines show the asymptotic behaviors. (b) $\langle h^2 \rangle$ as a function of the average linear system size $\tilde{L} = \sqrt{L_x L_y}$ compared to the scaling law $\langle h^2 \rangle = C_{2D} L^{2-\eta}$ with $C_{2D} = 0.0026$ and $\eta = 0.85$ (dashed line). Both axes are in logarithmic scale. This Figure has to be compared with the figs. 2 and 3 of Ref. 6.

Monte Carlo simulations for the honeycomb lattice.

The scaling laws described above have been obtained by analyzing the asymptotic behavior due to thermal fluctuations of continuous membranes. Recently, its validity was proven on a discrete 2D lattice, the graphene layer⁶. This was done with MC simulations using a potential suited for the Carbon compounds by adopting PBC on square samples. In fig. 2 we reproduce these results as a previous step before the study of the ribbons. Figure 2 (a) shows $q^2 H(q)/N$, which is the normal-normal correlation function because the unit vector normal to the surface \mathbf{n} is connected with h by $\mathbf{n} \approx \mathbf{e}_z - \nabla h$. It is calculated over 2D layers of several sizes as indicated on the plot. Besides this, fig. 2(b) shows $\langle h^2 \rangle$ as a function of the average linear system size $\tilde{L} = \sqrt{L_x L_y}$ compared to the eq. (7). These results were obtained through ordinary MC simulations including the wave-moves and using the quasi-harmonic (QH) potential introduced in Ref. 6. The details of the calculation, including the implementation of the wave-moves, follow the lines described in this reference. We have found the right acceptance range in the simulations by using amplitudes for wave-moves of the type $A = C_{wm}/\tilde{L}^{R_{scal}}$, with $C_{wm} = 0.01$ and $R_{scal} = 0.32$. The observed agreement should be taken as a check of the reliability of our sampling procedure.

From the previous section it is expected that when one of the dimensions of the square sample is reduced a distinct behavior should appear in the scaling of $\langle h^2 \rangle$, otherwise, $q^2 H(q)/N$ should show the same scaling. Figure 3 (a) shows that the asymptotic behavior of $q^2 H(q)/N$

remains valid starting from the square sample with $N=37888$ by reducing L_x as indicated (the same behavior is obtained by decreasing L_y). In fig. 3 (b) it can be observed that the scaling behavior of $\langle h^2 \rangle$ against \tilde{L} , corresponding to three different samples, is followed only for certain widths but it is not fulfilled when the sample becomes narrow enough. In all the cases we have verified that the same behavior is obtained by decreasing L_y .

As previously discussed we have adopted PBC in all the simulations. In this form we avoid edge reconstruction effects on the samples which could lead to unwanted effects for our study. We have limited the width of the studied ribbons to be large enough values in a way that bulk effects accounted by PBC are an important part of the physics of this problem.

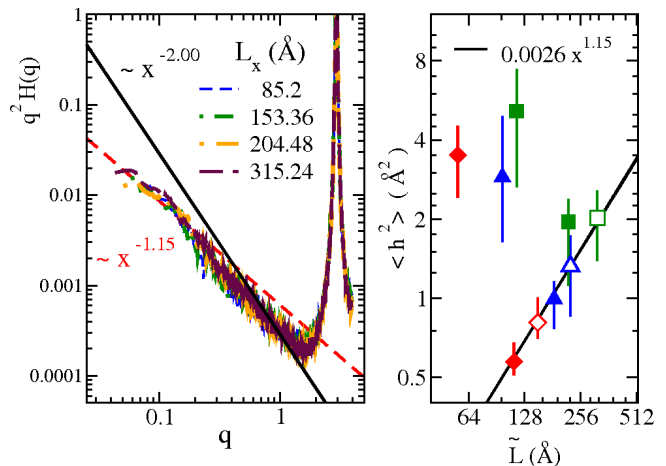


FIG. 3: (a) (Color online) $q^2 H(q)/N$ against q at $T = 300$ K calculated for different ribbon widths L_x , starting from the 2D $N = 37888$ ($L_x = 315.24\text{\AA}$) layer, as indicated on the plot. The asymptotic behavior remains valid independently of the ribbon width as was discussed previously in the text. (b) $\langle h^2 \rangle$ as a function of the average linear system size $\tilde{L} = \sqrt{L_x L_y}$ compared to the scaling law $\langle h^2 \rangle = C_{2D} L^{2-\eta}$ used in fig.2 (b). Open symbols correspond to square lattices, being square for $N = 37888$, triangle for $N = 19440$ and diamond for $N = 8640$. Filled symbols represent ribbon type lattices obtained from the square ones by reducing the L_x dimension. Starting from each 2D layer, in all cases the scaling law is broken at a certain value that we analyze further below. Both axes are in logarithmic scale.

The one-dimensional behavior. From fig. 3 (a) it can be established that the value of η does not change when going from the square membrane to a ribbon. Now, a similar analysis leading to Eq. 7 can be undertaken for the thin ribbons. In this case, the mean square fluctuations acquire a dependence toward the long direction L_y and the scaling laws become

$$\langle h^2 \rangle \sim \frac{L_y^{3-\eta}}{L_x}, \quad \langle \theta^2 \rangle \sim \frac{L_y^{1-\eta}}{L_x} \quad (8)$$

The main result of this work is present in fig. 4 where it

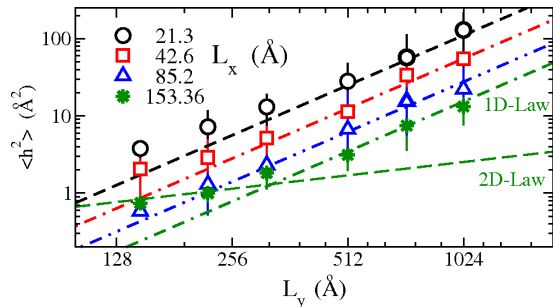


FIG. 4: (Color online) $\langle h^2 \rangle$ versus the longitude of the ribbon L_y for several ribbons width L_x as indicated. The dotted line serves to compared to the scaling law $\langle \langle h^2 \rangle \rangle = (C_{1D}/L_x)L_y^{3-\eta}$ with $C_{1D} = 0.0055$. The dashed line represent the 2D scaling for the widest ribbon (see the text). The crossover 2D to 1D can be seen clearly in this case. Both axis are in logarithmic scale.

can be observed the scaling of $\langle h^2 \rangle$ against L_y measured with the MC simulations for different ribbon widths as indicated. The comparison with the eq. (8) using the law $(C_{1D}/L_x)L_y^{3-\eta}$ with $C_{1D} = 0.0055$ shows an excellent agreement in all the cases for the larger values of L_y where the 1D aspect is stronger. The lowest L_y point of the $L_x = 153.36 \text{ \AA}$ sample (star symbol) corresponds to the 2D lattice $N=37888$ where, as we already discussed, the expectation value of fluctuations is described by Eq. (7). For this reason we also include on the plot this law using the fitted value $C_{2D} = 0.0026$, and $L_x = 153.36 \text{ \AA}$. This point is the only one included in this figure which corresponds to a 2D layer. The change of the scaling, thus, emerges clearly and the fittings allow us, by equaling both laws, Eq. (8) (1D) and Eq. (7) (2D), to estimate the ratio $R_{2D \leftrightarrow 1D}$ in which the crossover should take place as

$$R_{2D \leftrightarrow 1D} = \frac{L_y}{L_x} = \frac{C_{1D}^{2/(\eta-4)}}{C_{2D}} \approx 1.609 \quad (9)$$

Conclusions. The long range order on the ribbons is not restored by the inclusion of η since eq. (8) implies that $\langle \theta^2 \rangle$ remains unbounded in the thermodynamical limit and therefore the free thin ribbons are not stable against a crumpled transition. For the finite samples studied here this transition has not appeared. In the experimental situation, the free standing samples are always supported at the edges, hence the induced tension can provide room for a higher stabilization of the ribbons¹⁰.

As the QH potential employed here is softer than those ones best suited for graphene^{11,12}, to extend our conclusions to the graphene nanoribbons we emphasize that, $R_{2D \leftrightarrow 1D}$ could be greater than the estimated here. However we do not expect a qualitative change in the overall behavior which is related to general scaling arguments. Even more, the use of more realistic Carbon-Carbon potentials would be desirable in the studies where the edge reconstruction is taken into account in addition to thermal excited ripples or the more stable configurations of low number of Carbon atoms¹³. Finally, we remark that $R_{2D \leftrightarrow 1D}$ do not represent the limit in which the crumpled instability would disassemble the lattice, but instead, where the crossover takes place followed by the change on the scaling laws described here. A strong corrugation could imply big changes on the electronic spectra of the nanoribbons and may even result in gap openings on the electronic spectra¹⁴.

Acknowledgments. We thank D. Mastrogiuseppe for carefully reading our manuscript and A. Fasolino for helpful comments. This work was partially supported by PIP 11220090100392 of CONICET, and PICT 1647 and PICT R 1776 of the ANPCyT.

¹ K. S. Novoselov et al., Science **306**, 666 (2004); K. S. Novoselov et al., Nature **438**, 197 (2005).
² N. D. Mermin and H. Wagner, Phys. Rev. Lett. **17**, 1133 (1966).
³ D. Nelson, T. Piran and S. Weinberg, Statistical Mechanics of Membranes and Surface (World Scientific, Singapore, 2004).
⁴ J. C. Meyer, A. K. Geim, M. I. Katsnelson, K. S. Novoselov, T. J. Booth, and S. Roth, Nature **446**, 60 (2007).
⁵ A. Fasolino, J. H. Los, and M. I. Katsnelson, Nat. Mater. **6**, 858 (2007).
⁶ J. H. Los, M. I. Katsnelson, O. V. Yazyev, K. V. Zakharchenko, and A. Fasolino, Phys. Rev. B **80**, 121405 (2009).
⁷ F. L. Braghin and N. Hasselmann. Phys. Rev. B **82**, 035407 (2010).

⁸ E. V. Castro, H. Ochoa, M. I. Katsnelson, R. V. Gorbachev, D. C. Elias, K. S. Novoselov, A. K. Geim, and F. Guinea, Phys. Rev. Lett. **105**, 266601 (2010).
⁹ Le Doussal P, Radzihosvsky L. Phys. Rev. Lett. **69**, 1209 (1992).
¹⁰ M. Neek-Amal and F. M. Peeters, Phys. Rev. B **82**, 085432 (2010).
¹¹ D. Brenner, O. A. Shenderova, J. A. Harrison, S.J. Stuart, B. Ni and S. B. Sinnott, J. Phys. Condens Matter **14** 782 (2002).
¹² J. H. Los, L. M. Ghiringhelli, E. J. Meijer, and A. Fasolino, Phys. Rev. B **72**, 214102 (2005).
¹³ D. P. Kosimov, A. A. Dzhurakhalov, and F. M. Peeters, Phys. Rev. B **81**, 195414 (2010).
¹⁴ S. Costamagna, O. Hernandez and A. Dobry, Phys. Rev. B **81**, 115421 (2010).